Hydrol. Earth Syst. Sci. Discuss., 6, 6107–6134, 2009
www.hydrol-earth-syst-sci-discuss.net/6/6107/2009/

Hydrology and Earth System Sciences Discussions

Papers published in *Hydrology and Earth System Sciences Discussions* are under open-access review for the journal *Hydrology and Earth System Sciences*

Improving the rainfall rate estimation in the midstream of the Heihe River Basin using rain drop size distribution

G. Zhao, R. Chu, X. Li, T. Zhang, J. Shen, and Z. Wu

Laboratory for Climate Environment and Disasters of Western China, Cold and Arid Regions Enviromental and Engineering Research Institute, CAS, Lanzhou, 730000, Gansu, China

Received: 6 July 2009 – Accepted: 7 September 2009 – Published: 24 September 2009

Correspondence to: G. Zhao (guozh@lzb.ac.cn)

Published by Copernicus Publications on behalf of the European Geosciences Union.

Abstract

During the intensive observation period of the Watershed Allied Telemetry Experimental Research (WATER), a total of 1074 raindrop size distribution were measured by the Parsivel disdrometer, a latest state of the art optical laser instrument. Because of the limited observation data in Qinghai-Tibet Plateau, the modeling behavior was not well-done. We used raindrop size distributions to improve the rain rate estimator of meteorological radar, in order to obtain many accurate rain rate data in this area. We got the relationship between the terminal velocity of the rain drop and the diameter (mm) of a rain drop: $v(D)=4.67D^{0.53}$. Then four types of estimators for X-band polarimetric radar are examined. The simulation results show that the classical estimator $R(Z)$ is most sensitive to variations in DSD and the estimator R (K_{DP}, Z, Z_{DR}) is the best estimator for estimating the rain rate. The lowest sensitivity of the rain rate estimator R (K_{DP}, Z, Z_{DR}) to variations in DSD can be explained by the following facts. The difference in the forward-scattering amplitudes at horizontal and vertical polarizations, which contributes K_{DP}, is proportional to the 3rd power of the drop diameter. On the other hand, the exponent of the backscatter cross section, which contributes to Z, is proportional to the 6th power of the drop diameter. Because the rain rate R is proportional to the 3.57th power of the drop diameter, K_{DP} is less sensitive to DSD variations than Z.

1 Introduction

The quantitative estimation of rain rates using the meteorological radar has been one of main themes in radar meteorology and radar hydrology. The conventional single-polarized Doppler radar uses the measurement of radar reflectivity, radial velocity, and the storm structure to infer some aspects of hydrometeor types and amounts. The relationships between the rain rate R and the radar reflectivity factor Z (Z–R relations) have been widely used to estimate rainfall amounts. However, the classic rain estima-

HESSD

6, 6107–6134, 2009

tion method has many sources of error (e.g., Joss and Waldvogel, 1990; Collier, 1996). The sensitivity of Z–R relations to variations in raindrop size distributions (DSD) is the major source of error. Raindrop size distributions are determined by microphysical processes such as coalescence and breakup, condensation, evaporation, and melting of snowflakes, etc. DSD also changes in time and space, in correspondence with changes in the microphysical process in a given precipitation system. Battan (1973) got a total of 69 Z–R relationships to show that there was large variability in Z–R relationships caused by natural variations in DSD. Atlas et al. (1984) showed from an analysis of experimental drop size spectra that the average estimation error due to variations in DSD would be about 33%.

With the advent of dual-polarized radar techniques it is generally possible to achieve significantly higher accuracies in the estimation of hydrometeor types, and in some cases of hydrometeor amounts. In contrast to conventional radars, which use Z–R relationships to estimate rain rates, polarimetric radars use polarimetric parameters, such as differential reflectivity Z_{DR} and specific differential phase K_{DP}. Because of being less sensitive to natural variations in the DSD, the polarimetric parameters are used in improving the quantitative estimation of rain rates. Seliga and Bringi (1976) first showed that Z_{DR} could be used to retrieve rain drop size distributions and can improve rain rate estimation methods. The usage of differential phase to improve rain rate estimation was proposed theoretically (Seliga and Bringi, 1978) and is now recognized as an essential parameter for polarimetric radar measurements by Ryzhkov and Zrnic (1995,1996). Most research in the field of radar polarimetry as applied to rainfall parameter estimates has been performed for the radar wavelengths at S-band, such as Sachidananda and Zrnic (1986), Chandrasekar et al. (1990). There are the wavelengths of operational radars in many countries (e.g., the S-band Weather Svuveillance Radar-1988 Doppler (WSR-88D) network in the United States). Longer radar wavelengths (such as those at S-band) are the obvious choice for measurements in moderate and heavy rain because of low attenuation and backscatter phase shifts effects. Partial attenuation of radar signals is already a problem at C-band frequencies.

HESSD

6, 6107–6134, 2009

Research studies on the C-band wavelength were done by May et al. (1999), Carey et al. (2000), Keenan et al. (2001), and Bringi et al. (2001). Many researches and operational meteorological radars employ shorter wavelengths, such as those at X-band. The partial attenuation effects at X-band are more severe when compared with those at C-band, and account for these effects has been a significant problem for quantitative estimates of rainfall parameters based on reflectivity measurements at these wavelengths. Chandrasekar et al. (2002) analyzed the error structure at the X-band, using a similar method as Chandrasekar et al. (1990) and showed that the $R(K_{DP})$ was relatively insensitive to DSD variations. A unique dataset consisting of high-resolution polarimetric radar measurements and dense rain gauge and disdrometer observations collected in east-central Florida during the summer of 1998 was examined by Brandes et al. (2002). All of the above validation studies have shown that there is an improvement in rainfall estimation if a dual-polarization radar is used and polarimetric rainfall estimation techniques are more robust with respect to DSD variations than are the conventional $R(Z)$ relations. At the moment, however, there is no consensus on the degree of improvement and the choice of an optimal polarization relation. The most significant improvement was reported in the latest study in Oklahoma (Ryzhkov et al., 2002) using the $R(K_{DP}, Z_{DR})$ relation. Relatively modest improvement was observed in Florida (Brandes et al., 2002, 2003, 2004) with the best results obtained from the $R(Z, Z_{DR})$ relation.

Scattering simulation is the most adequate method for clarifying the effect of DSD variations. This method is used in studies done by Sachidananda and Zrnic (1986), Chandrasekar et al. (1990), and Matrosov et al. (1999). In this work we use three parameters distribution to study quantitatively the statistical errors of polarimetric rain rate estimatiors due to DSD variations, and use polarization radar parameters Z_{DR} and K_{DP} to improve the quantitative estimation of the rain rate.

2 Objectives of the experiment

The following scientific questions will be explored in this work.

1. The raindrop's terminal velocity is an important parameter in the microphysical process. The relationship between the terminal velocity and the raindrop size plays an important role in estimating the rain rate. This will be given in Sect. 4.2.

2. Although the relationships between the rain rate R and the radar reflectivity factor Z (Z–R relations) have been widely used to estimate rainfall amounts, they have many sources of error. Why Z–R relations are not one and only for rain rate estimating is also an important objective. The explanation will be given in Sect. 5.

3. The polarimetric parameters are used in improving the quantitative estimation of rain rates. We get four types of estimators with polarimetric parameters to explain the polarimetric radar is superior to conventional single-polarized Doppler radar in Sect. 6.

3 Experiment

The experiment area was carried out in the northeast of Qinghai-Tibet Plateau, (38.85° N, 100.41° E), and the altitude is 1515 m. This area is in the midstream of the Heihe basin. This basin is very important for the Northwestern China, because they are not only the bases of agriculture but also offer a better microclimatic environment for developing the ecosystem. The arid region of the basin is one of the main arid regions in the world and its mountain topography forms the particular sight pattern of "glacier-river-oasis-desert" which is linked by water. The raindrop size data were collected from May to July 2008, during the second part of the Watershed Airborne Telemetry Experimental Research (WATER) project.

The instrument used is OTT Parsivel made by Germans. The new generation of Parsivel disdrometer provides the latest state of the art optical laser technology. The

theory behind Parsivel is a laser sensor that produces a horizontal strip of light. The emitter and the receiver are integrated into a single protective housing. If there are no particles in the laser beam, the maximum voltage is output at the receiver. Precipitation particles passing through the laser beam block off a portion of the beam corresponding to their diameter, thus reduce the output voltage; this determines the particle size. To determine the particle speed, the duration of the signal is measured. A signal begins as soon as a precipitation particle enters the light strip and ends when it has completely left the light strip. Each hydrometeor, which falls through the measuring area, is measured simultaneously for size and velocity with an acquisition cycle of 50 kHz. It is subsequently classified into 32 classes of sizes and velocities. The basic measuring ranges from 0 to 20 m/s and 0.2 to 25 mm covering all natural precipitation types from drizzle, rain, mixed form, ice pellets, hail through to snow. Parsivel determines the exact precipitation type by internal spectrum signature comparison, using particle size and velocity distribution information. Even drops registering parabolic form in different signature classes will be corrected in shape in order to correlate to their ideal sphere and will be matched to their single water equivalent. Border events will be considered and corrected by statistical methods. The adjustable measuring interval from 10 s to 60 min coupled with fast data signal processing performance and features enable Parsivel to provide real-time and highly accurate intensity and accumulated precipitation data.

4 Equations and analysis methods

4.1 Equations for drop size distribution and drop shape

Ulbrich (1983) first report on an observed raindrop spectrum is well approximated by a three parameter gamma function of the form:

$$N = N_0 D^{\mu} \exp(-\Lambda D) \quad (1)$$

where N is also the number of drops per unit volume per unit size interval, N_0, Λ, μ, are the intercept parameter, the slope parameter, and the shape parameter, respectively.

The shape of a falling raindrop in still air is determined by a balance of three types of forces working on the drop surface, hydrostatic pressure, surface tension, and aerodynamic pressure. While a small drop has a spherical shape, and a larger drop tends to have an oblate spheroid shape with a slightly flatter base. This characteristic of raindrop shape is essential for polarimetric radar measurements of rainfall. The axis-ratio formulas used in the present study are:

$$\alpha = 1.0048 + 0.0057D_e - 2.628D_e^2 + 3.682D_e^3 - 1.677D_e^4, \quad (2)$$
$$D_e < 0.11\,\text{cm}, \quad D_e > 0.44\,\text{cm}$$

$$\alpha = 1.012 - 0.144D_e - 1.03D_e^2, \quad 0.11\,\text{cm} \le D_e \le 0.44\,\text{cm} \quad (3)$$

where D_e is the volume-equivalent spherical diameter (in centimeters). Equation (2) is for equilibrium axis ratios derived from the numerical model of Beard and Chuang (1987), and Eq. (3) is the axis ratio fit obtained from laboratory and field measurements by Andsager et al. (1999).

4.2 Rain rate and rain water content

When the drop size distribution is given, the rain rate R (mm h^{-1}) can be calculated by:

$$R = 0.6\pi \times 10^{-3} \int_{D_{min}}^{D_{max}} D^3 v(D) N(D) \mathrm{d}D, \quad (4)$$

where D is the diameter (mm) of a rain drop, D_{max} is the maximum drop diameter, $v_t(D)$ is the terminal velocity (m s^{-1}) of the drop in still air and $N(D)\mathrm{d}(D)$ the number of drops (m^{-3}) in the diameter interval D to D+dD. Table 1 is the terminal velocity of the rain drop with different diameters. Figure 1 shows the curves using the method

of least squares for the terminal velocity of the rain drop with different diameters. Get a relationship:$v(D)=4.67D^{0.53}$. Compare with the relationship: $v(D)=3.78D^{0.67}$ which got by Atlas (1977), we found that the terminal velocity of the rain drop in these areas is larger than Atlas's, that is because barometric pressure is lower and the air is thinner in this areas. This lead to little resistance during the rain drop fall in the air.

The rain water content M (kg m^{-3}) is given by:

$$M = \frac{\rho_w \pi}{6} \int_{D_{min}}^{D_{max}} D^3 N(D) \mathrm{d}D \,, \tag{5}$$

where ρ_w is the water density (10^3 kg m^{-3}). The rainwater content M is one of the important parameters in meteorology. The vertical distribution information of M is useful for understanding the evolution of precipitation processes in clouds. The vertical integrated liquid water content is a useful parameter for the very short-range forecasting of rainfall. On the larger scales, the change in M with height over a long period, is related to the latent heat release in the surrounding atmosphere, which will be an important heat source in global-scale circulation.

4.3 Polarimetric parameters

The reflectivity factor is defined by:

$$Z_{HV} = \frac{\lambda^4}{\pi^5} \left| \frac{m^2+1}{m^2-1} \right|^2 \int_{D_{min}}^{D_{max}} \sigma_{HV}(D) N(D) \mathrm{d}D \,, \tag{6}$$

where λ is the radar wavelength, m the complex refractive index of water, and σ_{HV} is the backscatter cross section at horizontal and vertical polarizations.

HESSD
6, 6107–6134, 2009

The differential reflectivity Z_{DR} (dB) is defined by:

$$Z_{DR} = 10\log\left(\frac{Z_H}{Z_V}\right) = 10\log\left(\frac{\int_{D_{min}}^{D_{max}} \sigma_H(D)N(D)\mathrm{d}D}{\int_{D_{min}}^{D_{max}} \sigma_V(D)N(D)\mathrm{d}D}\right). \quad (7)$$

The differential reflectivity Z_{DR} is a measure of the reflectivity-weighted mean axis ratio of the hydrometeors in a radar sampling volume which is defined by the radar beam width and the pulse width.

The specific differential phase K_{DP} (deg km^{-1}) is defined by:

$$K_{DP} = \frac{180}{\pi}\lambda \mathrm{Re}\int_0^{D_{max}} [f_H(D) - f_V(D)]N(D)\mathrm{d}D\,, \quad (8)$$

where Re refers to the real part of the integral, f_H and f_V are the forward-scattering amplitudes at horizontal (H) and vertical (V) polarizations, respectively.

5 Classic estimation methods of rain rate and rainwater content

The sensitivity to natural variations in DSD is a substantial source of error in classic estimators of rain rate R, and rain water content M. This is due to the fact that the R–Z relation (M–Z relation) is not a one to one relation; the same Z does not necessarily give the same R (M) and the same $R(M)$ does not necessarily give the same Z because Z and $R(M)$ depend on different moments of the DSD. Under Rayleigh scattering, Z is proportional to D^6 while R is proportional to $D^{3.53}$($v(D)$=4.67$D^{0.53}$) and M is proportional to D^3. These facts can be explained by way of the observed DSD examples shown in Fig. 1a which has the same Z values (35.5 dBZ) but different rain rates

(4.3, 6.7, and 8.0 mm h^{-1}). The differences in the rain rate are due to the difference in the drop density of smaller drops; the DSD sample of R=8.0 mm h^{-1} has a larger number of drops for D=1–3 mm compared to the other DSD samples. Figure 1b shows three examples of drop size distributions that have the same rain rate R (0.2 mm h^{-1}), but different reflectivity factors Z (13, 15, and 16 dBZ). In contrast to the case of the rain rate, the difference in reflectivity factors can be explained by the difference in the number density of larger drops; the DSD sample of Z=16 dBZ has the larger number density for the drops D>1.5 mm. This opposite dependency of R and Z on drop size D is due to the fact that Z is proportional to D^6, while R is proportional to $D^{3.53}$.

R and Z are dependent on different moments of the DSD. Thus, natural variations in DSD cause large dispersions in R–Z scatter plots. Classifying rain type (convective and stratiform rain) is one of the useful techniques for improving the accuracy of classic estimators $R(Z)$ and $M(Z)$. Scatter plots of R–Z and M–Z relations are shown in Figs. 3 and 4, respectively, where y-axis taking logarithm, for convective and stratiform rain. R and M of each point are calculated directly from 30 s-averaged DSD. Scatter plots of R–Z relations are shown in Fig. 3, where y-axis taking logarithm. From Fig. 3, we found R and Z obey the relationship: $R=a\times10^{b\times Z}$. The obtained R–Z relations for stratiform rain, convective rain, and all rain types are $R=3.2\times10^{-2}\times10^{0.058\times Z}$, $R=4.6\times10^{-2}\times10^{0.056\times Z}$, and $R=3.0\times10^{-2}\times10^{0.06\times Z}$, respectively. AS for the rain water content M, the obtained M–Z relations for stratiform rain, convective rain, and all rain types are $M=1.0\times10^{-3}\times10^{0.064\times Z}$, $M=7.9\times10^{-4}\times10^{0.069\times Z}$, and $M=9.6\times10^{-4}\times10^{0.067\times Z}$, respectively.

Several combinations of polarimetric variables are possible for constructing rain rate estimators. The simplest method is an estimator which uses only K_{DP}. Scatter plots of R–K_{DP} and M–K_{DP} relations are shown in Figs. 5 and 6, respectively, for stratiform rain and convective rain. From Fig. 5, we found R and K_{DP} obey the relationship: $R=a+bK_{DP}$. The obtained R–K_{DP} relations for stratiform rain and convective rain are $R=0.07907+1.74788K_{DP}$ and $R=0.027+2.122K_{DP}$, respectively. AS for the rain water

content M, the obtained $M-K_{DP}$ relations for stratiform rain and convective rain are $M=0.002+0.074K_{DP}$ and $M=-0.008+0.111K_{DP}$, respectively.

It has been recognized for a long time that the X-band wavelength was not useful for accurate rainfall measurements because of the rain attenuation problem of Z. However, this situation changed dramatically after polarimetric radar, which measures differential phase and the specific differential phase K_{DP}, became available. In addition to the less sensitivity of differential phase to DSD variations, it is immune to radar hardware calibration problems, which are one of the major sources of error for signal power measurements and also immune to rain attenuation. Differential phase measurements are little affected by the presence of hail, which causes overestimation of the rain rate in the case of classic $R(Z)$ estimator. The differential phase can be used to correct the reflectivity factor for loss due to beam blockage by topography, attenuation, and anomalous propagations (Ryzhkov and Zrnic, 1996; Ryzhkov et al., 2000). Because of these advantages, it is important to construct rain estimators using a combination of polarimetric variables such as $R(Z, Z_{DR})$ and $R(K_{DP}, Z, Z_{DR})$. So we use the relationships: $R=a\times10^{b\times Z-c\times Zdr}$ and $R=a\times K_{DP}^{b}\times10^{c\times Z-d\times Zdr}$. A non-linear regression analysis was applied to the data to obtain the coefficients of these estimators. The results are shown in Tables 2a and b. Analyses and discussions similar to those for the rain rate estimators were applied to estimations of rain water content (M) using polarimetric radar variables. The results are summarized in Tables 3a and b.

Comparisons of rain rates R calculated from estimators $R(Z)$, $R(K_{DP})$, R (Z, Z_{DR}) and R (K_{DP}, Z, Z_{DR}) with rain rates R_{cal} calculated from observed raindrop size spectra are shown in Figs. 7 and 8 for stratiform rain and convective rain, respectively. Scatter plots suggest that, of the four estimators, R (K_{DP}, Z, Z_{DR}) is the most accurate estimator from the viewpoint of the insensitiveness to variations in DSD. The worst estimator is $R(Z)$, which is most sensitive to variations in DSD.

To quantitatively examine the uncertainty of the four estimators, $R(Z)$, R (K_{DP}), $R(Z, Z_{DR})$ and R (K_{DP}, Z, Z_{DR}), due to the variations in DSD, two types of error were calculated: the normalized error (NE), the percentage root-mean-squared error (PRMSE).

HESSD
6, 6107–6134, 2009

These errors are defined as:

$$\mathrm{NE} = \langle |R_{\mathrm{est}} - R_{\mathrm{dis}}| \rangle / \langle R_{\mathrm{dis}} \rangle \,, \tag{9}$$

$$\mathrm{PRMSE} = \left\langle \sqrt{(R_{\mathrm{est}} - R_{\mathrm{dis}})^2} / R_{\mathrm{dis}} \right\rangle \,. \tag{10}$$

The NE of $R(Z)$, R (K_{DP}), $R(Z, Z_{\mathrm{DR}})$ and R ($K_{\mathrm{DP}}, Z, Z_{\mathrm{DR}}$) for stratiform rain are 32.0, 18.2, 15.0, and 12.3%, respectively. The NE of $R(Z)$, R (K_{DP}), $R(Z, Z_{\mathrm{DR}})$ and R ($K_{\mathrm{DP}}, Z, Z_{\mathrm{DR}}$) for convective rain are 28.8, 16.8, 14.2, and 11.3%, respectively. The PRMSE of $R(Z)$, R (K_{DP}), $R(Z, Z_{\mathrm{DR}})$ and R ($K_{\mathrm{DP}}, Z, Z_{\mathrm{DR}}$) for stratiform rain are 33.2, 19.1, 15.1, and 13.3%, respectively. The PRMSE of $R(Z)$, R (K_{DP}), $R(Z, Z_{\mathrm{DR}})$ and R ($K_{\mathrm{DP}}, Z, Z_{\mathrm{DR}}$) for convective rain are 30.8, 16.9, 14.0, and 10.3%, respectively. From these comparisons, we can conclude that R ($K_{\mathrm{DP}}, Z, Z_{\mathrm{DR}}$) is the least sensitive to variations in DSD.

Although error analysis based on the comparisons of radar estimates with gauge measurements is not necessarily an appropriate method to confirm the sensitivity of rain rate estimators to variations in DSD, it may be useful to know the total performance of rain rate estimators. The values of errors obtained from the radar-gauge analysis are usually larger than those of the simulation because error sources other than DSD variations can be commonly introduced: for example, errors due to the difference in time and space for measurements, due to evaporation, or due to attenuation correction of Z and Z_{DR}. From the comparison of radar estimated rainfall amount with rain gauge data, Park et al. (2005) showed that the NE of attenuation corrected $R(Z)$, and the NE of $R(K_{\mathrm{DP}})$ are 26%, and 21%, respectively for 15-min rainfall accumulations and 19 and 11%, respectively for one-hour rainfall accumulations.

6 Summary

The present study used a total of 1074 thirty second-averaged raindrop size spectra, measured with a Parsivel disdrometer to calculate the radar reflectivity factor Z, the

specific differential phase K_{DP}, and the differential reflectivity Z_{DR}. Then we get four types of rain rate estimators $R(Z)$, $R(K_{DP})$, $R(Z, Z_{DR})$ and $R(K_{DP}, Z, Z_{DR})$ with these parameters. We quantify the sensitivity of four types of rain rate estimators to natural variations in DSD. Most of the previous studies evaluated polarimetric estimators, comparing radar estimates with surface gauge measurements. It is well known that the difference between radar estimates and rain gauge data is due not only to the accuracy of the rain rate estimator to variations in DSD, but also to other factors, such as differences in the sampling volume size, differences in the observation height, accuracy of the radar system calibration, etc. The results of our simulations show that the estimator $R(K_{DP}, Z, Z_{DR})$ is less sensitive to natural variations in DSD than the classical estimator $R(Z)$. The normalized errors (NEs) of $R(Z)$ and $R(K_{DP}, Z, Z_{DR})$ for stratiform rain and convective rain are 32.0, 12.3 and 28.8%, 11.3%, respectively. The percentage root-mean-squared error (PRMSE) which is also used to quantify the statistical error of stratiform rain and convective rain are 33.2, 13.3, and 30.8%, 10.3%, respectively. The lower sensitivity of $R(K_{DP}, Z, Z_{DR})$ and the higher sensitivity of $R(Z)$ to variations in DSD can be explained by the fact that the difference between the forward-scattering amplitudes at horizontal (H) and vertical (V) polarizations $f_H(D) - f_V(D)$ in the definition of K_{DP} is proportional to the 3rd power of the diameter of a raindrop for the monodisperse DSD model, while the reflectivity factor Z is proportional to the 6th power of the diameter.

Acknowledgement. This work is supported by the CAS (Chinese Academy of Sciences) Action Plan for West Development Project "Watershed Airborne Telemetry Experimental Research (WATER)" (Grant No.: KZCX2-XB2-09) and the National Natural Science Foundation of China (Grant No.: 40575008).

References

Atlas, D., Ulbrich, C. W., and Meneghini, R.: The multi-parameter remote measurement of rainfall, Radio Sci., 19, 3–22, 1984.

Andsager, K., Beard, K. V., and Laird, N. F.: Laboratory measurements of axis ratios for large drops, J. Atmos. Sci., 56, 2673–2683, 1999.
Battan, L. J.: Radar Observation of the Atmosphere, Univ. Chicago Press, p. 324, 1973.
Beard, K. V. and Chuang, C.: A new model for the equilibrium shape of raindrops, J. Atmos. Sci., 44, 1509–1524, 1987.
Brandes, E. A., Zhang, G., and Vivekanandan, J.: An evaluation of a drop distribution based polarimetric radar rainfall estimator, J. Appl. Meteorol., 42, 652–660, 2003.
Brandes, E. A., Zhang, G., and Vivekanandan, J.: Drop-size distribution retrieval with polarimetric radar: model and application, J. Appl. Meteorol., 43(3), 461–475, 2004.
Brandes, E. A., Zhang, G., and Vivekanandan, J.: Experiments in rainfall estimation with polarimetric radar in a subtropical environment, J. Appl. Meteorol., 41, 674–685, 2002.
Bringi, V. N. and Chandrasekar, V.: Polarimetric Doppler Weather Radar, Cambridge Univ. Press, p. 636, 2001.
Carey, L. C., Rutledge, S. A., Ahijevych, D. A., and Keenan, T. D.: Correcting propagation effects in C-band polarimetric radar observations of tropical convection using differential propagation phase, J. Appl. Meteorol., 39, 1405–1433, 2000.
Chandrasekar, V., Bringi, V. N., Balakrishnan, N., and Zrnic, D. S.: Error structure of multiparameter radar and surface measurements of rainfall. Part III: Specific differential phase, J. Atmos. Oceanic Technol., 7, 621–629, 1990.
Chandrasekar, V., Gorgucci, E., and Bringi, V. N.: Evaluation of polarimetric radar rainfall algorithms at X-band, Proc. 2nd European Conf. on Radar Meteorology (ERAD), Delft, Netherlands, 277–281, 2002.
Collier, C. G.: Applications of Weather Radar Systems. A Guide to Uses of Radar Data in Meteorology and Hydrology, 2nd edn., John Wiley & Sons, p. 390, 1996.
Joss, J. and Waldvogel, A.: Precipitation measurements and hydrology. Radar in Meteorology, D. Atlas, Ed., Amer. Meteorol. Soc., 577–606, 1990.
Keenan, T. D., Zrnic, D. S., Carey, L., and May, P.: Sensitivity of 5-cm wavelength polarimetric radar variables to raindrop axial ratio and drop size distribution, J. Appl. Meteorol., 40, 526–545, 2001.
Matrosov, S. Y., Kropfli, R. A., Reinking, R. F., and Martner, B. E.: Prospects for measuring rainfall using propagation differential phase in X- and Ka-radar bands, J. Appl. Meteorol., 38, 766–776, 1999.
May, P. T., Keenan, T. D., Zrnic, D. S., Carey, L. D., and Rutledge, S. A.: Polarimetric radar

measurements of tropical rain at a 5-cm wavelength, J. Appl. Meteorol., 38, 750–765, 1999.
Park, S.-G., Maki, M., Iwanami, K., Bringi, V. N., and Chandrasekar, V.: Correction of radar reflectivity and differential reflectivity for rain attenuation at X-band. Part II: Evaluation and application, J. Atmos. Oceanic Technol., 22(11), 1633–1655, 2005.
Ryzhkov, A. V. and Zrnic, D. S.: Comparison of dual-polarization radar estimators of rain, J. Atmos. Oceanic Technol., 12, 249–256.465, 1995.
Ryzhkov, A. V. and Zrnic, D. S.: Assessment of rainfall measurement that uses specific differential phase, J. Appl. Meteorol., 35, 2080–2090, 1996.
Ryzhkov, A. V., Zrnic, D. S., and Fulton, R.: Areal rainfall estimates using differential phase, J. Appl. Meteorol., 39, 263–268, 2000.
Ryzhkov, A. V., Schuur, T. J., and Zrnic, D. S.: Testing a polarimetric rainfall algorithm and comparison with a dense network of rain gauges, Hydrological Resources on Hydrological Applications of Weather Radar, Kyoto, Japan, 159–164, 2002.
Sachidananda, M. and Zrnic, D. S.: Differential propagation phase shift and rainfall rate estimation, Radio Sci., 21, 235–247, 1986.
Seliga, T. A. and Bringi, V. N.: Potential use of radar differential reflectivity measurements at orthogonal polarizations for measuring precipitation, J. Appl. Meteorol., 15, 69–76, 1976.
Seliga, T. A. and Bringi, V. N.: Differential reflectivity and differential phase shift: Applications in radar meteorology, Radio Sci., 13, 271–275, 1978.
Ulbrich, C. W.: Natural variations in the anslytical form of the raindrop size distrution, J. Climate Appl. Meteorol. 22, 1764–1775, 1983.

Table 1. The terminal velocity of the rain drop with different diameter.

D (mm)	0.31	0.44	0.56	0.68	0.81	1.19	1.63	2.13	2.38	4.25
V ($m\,s^{-1}$)	2.6	3.0	3.4	3.8	4.4	5.2	6.0	6.8	7.6	10.4

Table 2a. Coefficients of the $R(Z, Z_{DR})$.

Rain type	a	b	c
Stratiform	0.026	0.083	–0.561
Convective	0.018	0.076	–0.155

HESSD

6, 6107–6134, 2009

Table 2b. Coefficients of the R (K_{DP}, Z, Z_{DR}).

Rain type	a	b	c	d
Stratiform	0.009	–0.173	0.103	–0.653
Convective	0.198	0.4405	0.035	–0.036

HESSD

6, 6107–6134, 2009

Table 3a. Coefficients of the $M(Z, Z_{DR})$.

Rain type	a	b	c
Stratiform	0.026	0.083	–0.561
Convective	0.018	0.076	–0.155

HESSD

6, 6107–6134, 2009

Table 3b. Coefficients of the $M(K_{DP}, Z, Z_{DR})$.

Rain type	a	b	c	d
Stratiform	0.009	–0.173	0.103	–0.653
Convective	0.198	0.4405	0.035	–0.036

HESSD

6, 6107–6134, 2009

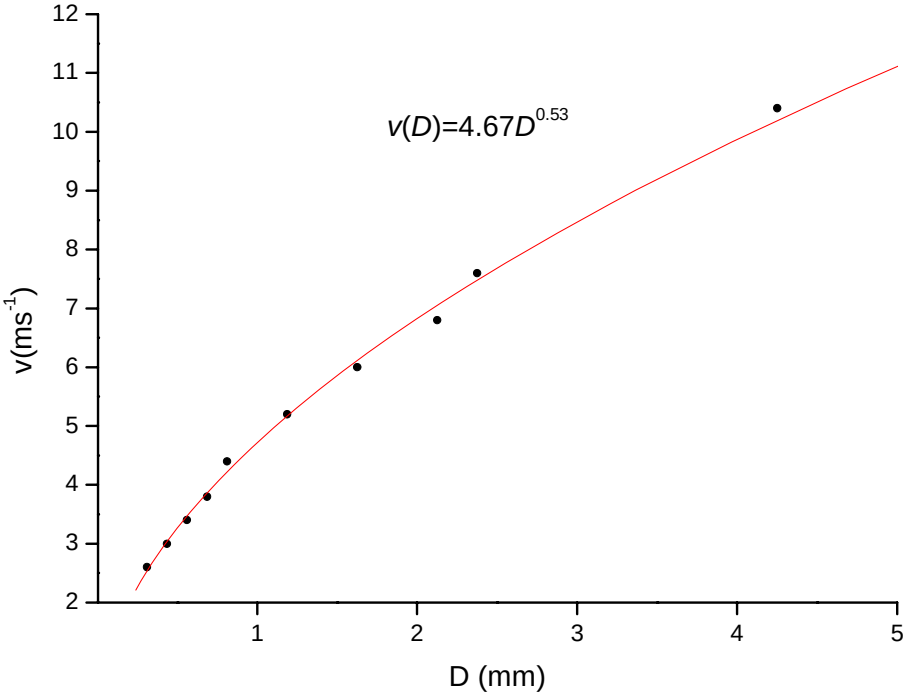

Fig. 1. The relationship between the rain drop diameter and the terminal velocity of the rain drop.

HESSD

6, 6107–6134, 2009

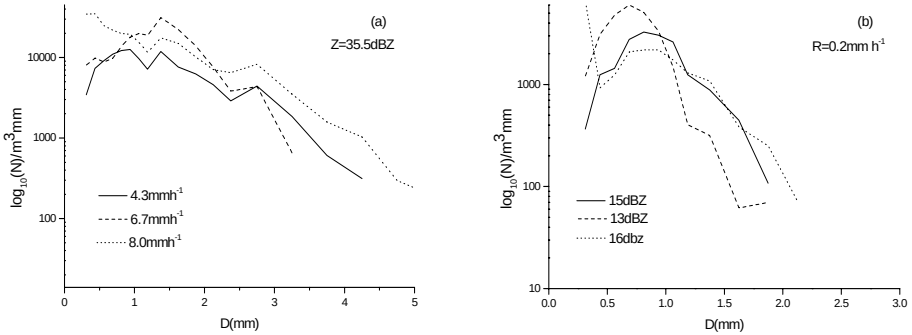

Fig. 2. The influence to the Z–R relationship by the changing of rain drop distribution.

HESSD
6, 6107–6134, 2009

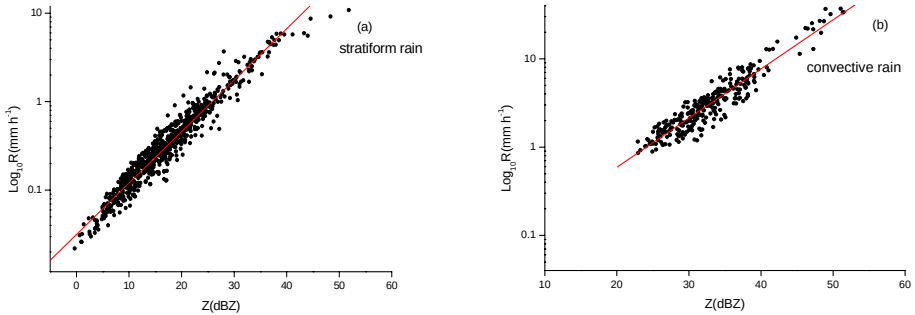

Fig. 3. Scatter plots of the radar reflectivity (Z) and the rain rate (R).

HESSD
6, 6107–6134, 2009

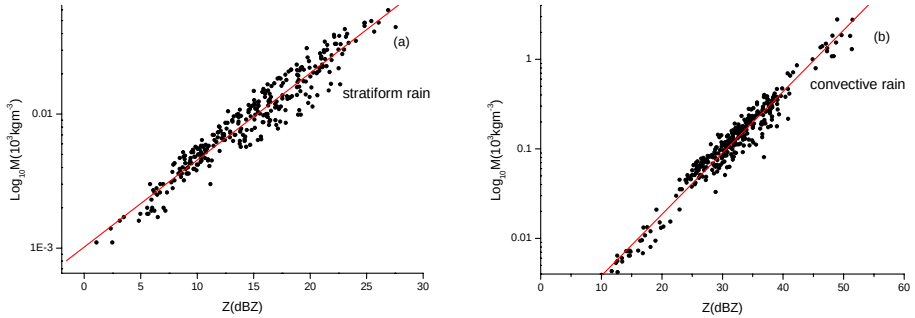

Fig. 4. Scatter plots of the radar reflectivity (Z) and the rain water content (M).

HESSD
6, 6107–6134, 2009

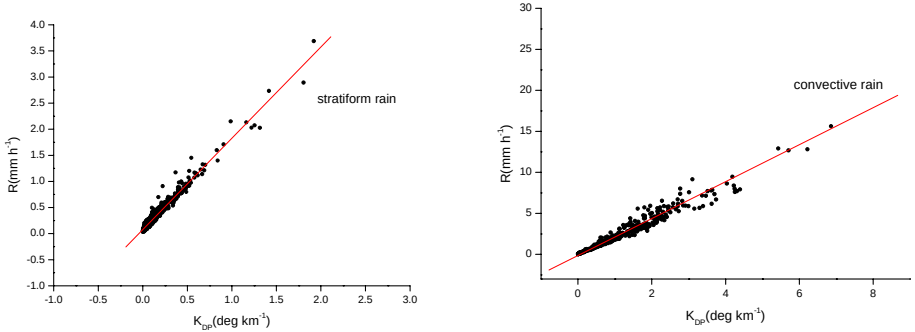

Fig. 5. Scatter plots of the specific differential phase (K_{DP}) and the rain rate (R).

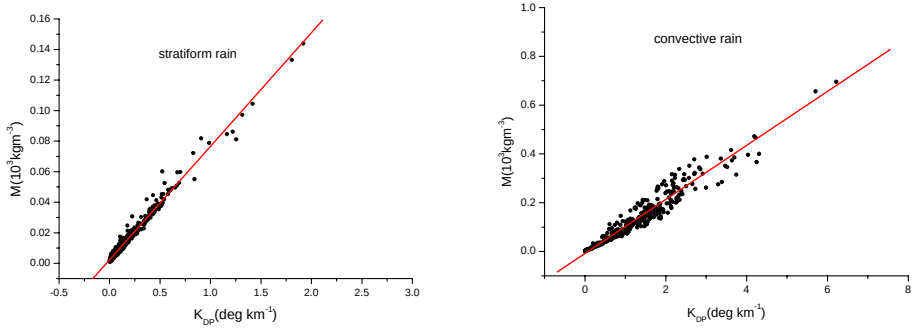

Fig. 6. Scatter plots of the specific differential phase (K_{DP}) and the rain water content (M).

HESSD
6, 6107–6134, 2009

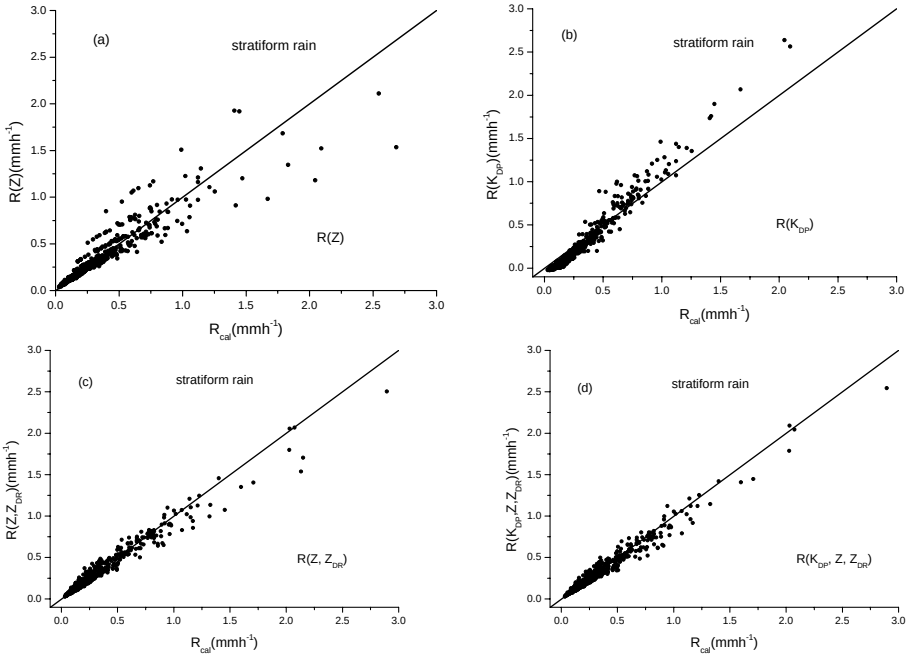

Fig. 7. Scatter plots of R_{cal} calculated from measured drop size distribution and R estimated by four types for rain rate estimators **(a)** $R(Z)$, **(b)** $R\ (K_{DP})$, **(c)** $R(Z, Z_{DR})$ **(d)** $R\ (K_{DP}, Z, Z_{DR})$.

HESSD
6, 6107–6134, 2009

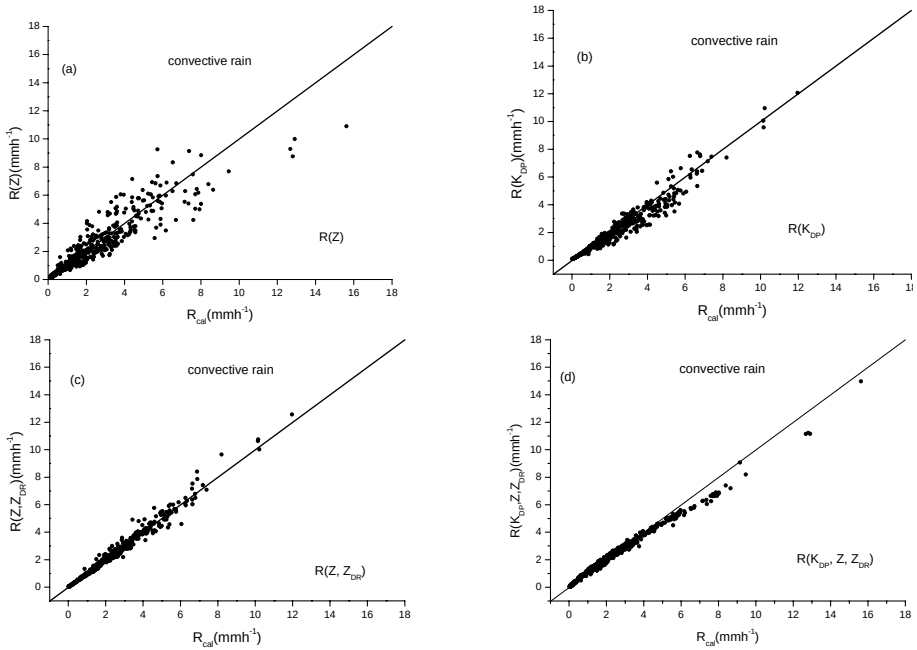

Fig. 8. Scatter plots of R_{cal} calculated from measured drop size distribution and R estimated by four types for rain rate estimators **(a)** $R(Z)$, **(b)** $R\ (K_{DP})$, **(c)** $R(Z, Z_{DR})$ **(d)** $R\ (K_{DP}, Z, Z_{DR})$.

HESSD
6, 6107–6134, 2009